J. Integr. Sci. Technol. 2024, 12(1), 703 Article

Journal of Integrated
SCIENCE & TECHNOLOGY

Performance comparison of different Wavelet based image fusion techniques for Lumbar Spine Images

Manan Nanavati,[1*] Mehul Shah[2]

[1]*Biomedical Engineering Department, Government Engineering College, Sector - 28, Gandhinagar, Gujarat, India.*
[2]*Instrumentation and Conrol Engineering Department, Vishwakarma Government Engineering College, Chandkheda, Ahmedabad, Gujarat, India.*

Received on: 02-Jun-2023, Accepted and Published on: 04-Aug-2023

ABSTRACT

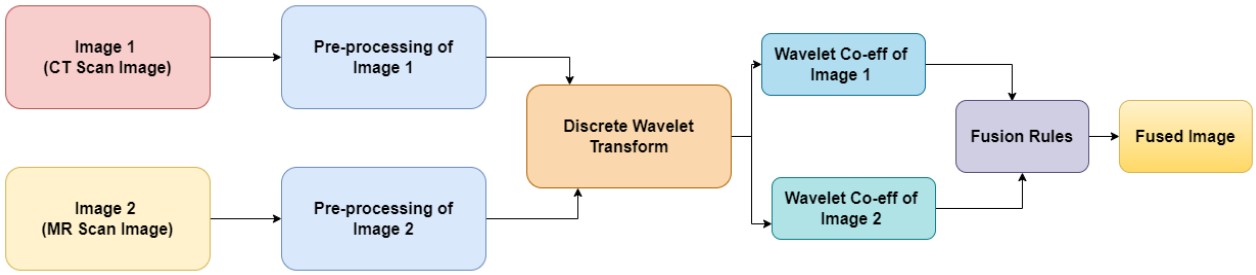

Image fusion of medical images gives an output representative image that contains more detail than each of the source images, making it an informative medium for clinicians. The main goal of multimodal image fusion is to act as a clinically supportive tool for a better and more accurate diagnosis, so that important information or features are considered. This work is aimed to implement and analyze Discrete Wavelet Transform (DWT) based Image fusion algorithm applied to the Computed Tomography (CT) and Magnetic Resonance Imaging (MRI) images of the lumbar spine. The information available from CT and MRI images totally complements each other, where the former is better for visualization of bony structures and the latter is better for visualization of soft tissues and nerves. Hence, the implemented algorithm effectively uses the information present in CT and MRI images and provides a resultant fuse image that can be used further for diagnosis and treatment planning. The performance analysis of the implemented DWT based image fusion algorithm is evaluated by quantitative quality metrics such as Entropy, $Q^{AB/F}$, mutual information, and spatial frequency and also tested under conditions like varying the parameters such as the types of wavelets used for decomposing the input images and the number of decomposition levels. The overall comparison of the majority of metrics has shown that the higher decomposition value in the wavelet of each family performs better in all of the cases presented in the study.

Keywords: Discrete wavelet transform, Level of decomposition, Lumbar spine, Medical image fusion

INTRODUCTION

Image fusion focuses on combining features and information of two or more images into one resultant image; e.g., in the case of multifocus images, it creates a single output image by combining the images taken by a different camera with different focus parameters,[1] and in the case of medical image fusion, it integrates images (usually two or more) having information about the same part of the body into one clear image. In recent times, the fusion of medical images has gained popularity. In the field of medical imaging, Magnetic Resonance Imaging (MRI), Computed Tomography (CT), Positron Emission Tomography (PET), and Single Photon Emission Computed Tomography (SPECT) are widely used imaging modalities that give information about the internal structure of the body in different aspects, which is helpful for clinical diagnosis for medical practitioners. Fusing images from different modalities gives as much information about the targeted body part of the diagnosis as possible, which resembles the reason

*Corresponding Author: Manan Nanavati, Research Scholar, Gujarat Technological University. Dr. Mehul Shah, Research Supervisor, Gujarat Technological University
Email: manan.2507@gmail.com, mkshah2000@gmail.com

Cite as: *J. Integr. Sci. Technol., 2024, 12(1), 703.*
URN:NBN:sciencein.jist.2024.v12.703

 ISSN: 2321-4635
http://pubs.thesciencein.org/jist

that usually surgeons or clinicians require images from different modalities for a better and more accurate diagnosis.

CT and MRI are widely used imaging modalities for diagnosis or screening purposes. A CT scan using an array of X-Ray sensors gives information about bony structures or hard tissues, whereas a MRI using a magnetic field gives information about soft tissues, organs, and blood vessels.[2,3] As mentioned, CT and MRI imaging outputs are totally complementary to each other. As a CT scan image cannot give information about ligament scars, tumors, or other soft tissue damages, and a MRI scan image fails to give details of bones, combining the information of MRI and CT may give details of bony structure as well as soft tissues in a single output image, which at the end can be helpful for better clinical diagnosis or treatment planning.

Image fusion methods are mainly classified into the following different types: pixel level[4], feature level,[5] and decision level.[6] Pixel level image fusion is preferred over the other two because of its good ability to preserve the original pixel value. Pixel level methods are further classified into two subtypes: spatial domain methods and transform domain methods. The spatial level methods include minimum, maximum, min-max, averaging, weighted average.[7] HIS,[8] Principal Component Analysis (PCA),[9] Brovey,[10] and pyramid based fusion methods[11] like local Gaussian Pyramid and Laplacian Pyramid[12-14] Gradient Pyramid,[15] and ratio of Low pass Pyramid.[16] Transform based methods basically work in the frequency domain, and it include methods like Wavelet Transform (WT) or using wavelets.[17-20] Discrete Cosine Transform (DCT),[21] Discrete Fourier Transform (DFT),[21] Stationary wavelet Transform (SWT),[22-24] Curvelet transform (CVT).[25] The main advantage of using wavelet based approaches over Fourier transform is that wavelets allow complex information, such as patterns and images, to be decomposed at different levels in its elementary form with high precision.

The pixel level method is preferred in the majority of image fusion applications, as it can preserve the pixel values, is time efficient, and its implementation is easier compared to the other two methods.

Different image fusion techniques have been proposed in the past decade, and a comparative study comparing various aspects is presented in different reports.[26-29] In reports by Cheng et.al.,[30] an image fusion algorithm using DWT was proposed for medical images. In report by Nawaz et.al.,[31] a novel algorithm for fusion of PET and CT images using the quaternion Discrete Fourier transform (DFT) using a weighted fusion rule was proposed. In report by Kavitha et.al.,[32] a fusion approach for MR and CT images using DWT and Ripplet transform was proposed. In a report by Doke et.al.,[33] a comparative image fusion study was presented for PET and CT images using eight different wavelets.

This paper implements discrete wavelet transform based image fusion and also analyzes the performance, especially focusing on the wavelets used for decomposition and the level of decomposition when applied to pairs of input CT and MR images of the lumbar spine.

The The rest of the paper is organized as follows: Section II explains the basics of image fusion and the need for an image registration process, and Section III presents the concepts of fusion using wavelets and its implementation. Section IV describes the experimental setup and dataset used in this work, along with the results of the implemented algorithms under different conditions and their comparison using quantitative analysis. Section V describes the analysis of the results, and the last section describes the overall summary.

IMAGE FUSION

The main goal of the image fusion process is to combine the information of two or more images into a single image while preserving the necessary information from the source images. Particularly in medical applications, the fusion of images from different modalities is preferable to having information from multiple images in a single representative image. Image fusion basically involves three major steps: (i) image registration; (ii) pre-processing of images; (iii) applying an image fusion algorithm.

Image registration is a process that involves overlaying and aligning two or more images with each other that are taken from different points, sources, and/or times while keeping one image as a fixed or reference image.[34] The main purpose of image registration is to geometrically align two different images for further processing towards the end goal of image fusion. In this work, the MR image and CT image are captured from different sensors of the same body part and from different viewpoints; hence, the image fusion process is not possible unless the two images are geometrically aligned with each other. The main classification of methods for image registration is: (i) Extrinsic image registration, based on foreign objects introduced in imaged space; (ii) Intrinsic image registration - based on image information generated by the patient/subject.[35,36] Intrinsic image registration is a more popular approach for registering images in clinical applications.[37] For image registration using intrinsic methods, it requires points or landmarks, curves, and gray levels of images. Intrinsic image registration techniques are further categorized into: (i) landmark based (ii) surface based and (iii) voxel based.

In this paper, the landmark based (also known as control point mapping) intrinsic approach is used as a method for registering CT and MR images, as the used dataset contains very few pairs of images. For simplicity, in this study, the dimensions of the input pair of images are the same. The study can be done in the future for image fusion and image registration for images with different dimensions. The landmark based registration involves users manually selecting the landmark points or control points in the pair of input images. By getting the positions of the landmark points, geometric transformations like affine, projective, or polynomial geometric transforms are applied further to the input images. The main advantage of landmark based image registration is that it focuses on the specific features or points selected by the user rather than automatically registering the image based on all the features. For image fusion of the lumbar spine, the landmark areas or focus areas are the alignment of the disc, degeneration of the disc, and vertebrae (s). The major steps involved in image registration using landmark points are:

- Selection of the moving image and the fixed image
- Selection of the landmark points
- Fine tuning of the selected landmark points

- Select and apply the appropriate transform method to get the registered image

In the pre-processing step, mainly the brightness and contrast stretching for the source CT and MR images are done. The main purpose of pre-processing is to match the level of contrast for a better fusion outcome and is also done due to the source image being taken from different sensors at different angles or heights.

Image fusion is further categorized into three different methods: (i) pixel level, (ii) feature level, and (iii) decision level.[38] Pixel level image fusion directly uses the information from source images at individual pixel levels and performs the image fusion. The feature level fusion mainly focuses on extracting features such as edges, pixel intensities, and image texture from the source images and merging them with relevant algorithms into one image.[39,40] In decision level fusion, the information is extracted from the source images one at a time.[39] According to various studies involved in medical image fusion, the application of pixel level fusion is more prevalent than that of the other two. The pixel level image fusion technique is further classified into (i) spatial domain based techniques and (ii) frequency domain based techniques, and its subclassification is described in Figure 01.

The spatial domain specifically deals with the pixels, and values are altered with different mathematical processes to get the desired fused image by combining all fused pixels. In the case of the frequency domain based technique, which is also referred to as the transform domain based technique in various literature, the source image is first converted into its corresponding frequency domain using any transform method, and further fusion is done. In this paper, the main focus is on the implementation of discrete wavelet transform based algorithms, which belong to the transform based technique and were tested under the conditions described in Section IV.

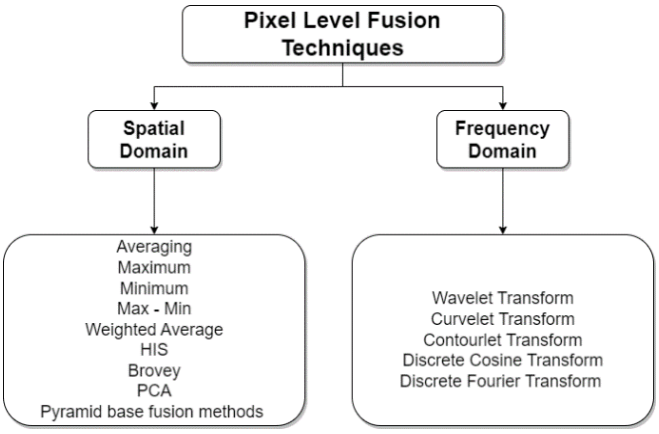

Figure 1: Classification of Pixel Level Fusion Technique

Image Fusion Using Discrete Wavelet Transform

The wavelet transform is one of the most commonly used techniques for image registration and image fusion[41-45]. Wavelets are effective tools for extracting information such as breakdown points, trends, and discontinuities at higher derivatives that other tools could not visualize easily. They are also effectively used for compression and de-noising without any loss of significant information. Hence, wavelets are widely used in handling medical imaging data for analysis. Wavelet transforms are mainly categorized into two main categories: (i) Continuous Wavelet Transform and (ii) Discrete Wavelet Transform. In this paper, the focus is on the application of the Wavelet Transform. The main concept of the Wavelet Transform (DWT) is to decompose the signal, with each level having a coarser level or being further divided into low frequency and high frequency bands. In the case of DWT applied to a 2D image, the decomposition takes place layer by layer on the input image, or in other words, 1-D DWT is first performed on the rows and then on the columns of the input image, resulting in four frequency bands (i) Low - Low (LL), (ii) Low - High (LH), (iii) High - Low (HL), and (iv) High - High (HH) at the first decomposition level. Figure 02 shows the first level of decomposition using DWT on the input image resulting in four subbands bands LL, LH, HL, and HH and the fusion of the respective bands. Similarly, for the nth level of decomposition, it will result in 3N + 1 frequency bands, out of which 3N bands represent the high frequency bands and the remaining will be the LL band of the input image.

The main steps for the image fusion using DWT based algorithm are as follows:

Step - 1: Image registration of input images, so that the corresponding pixel or region of the image is aligned geometrically with each other.

Step - 2: Application of DWT to the input images to get decomposed images. The transformed image contains one low frequency band (LL band) and three high frequency bands (LH, HL, and HH bands).

Step - 3: The wavelet coefficients of input images are fused in such a way that the low frequency bands of each input image are fused with a fusion rule and the high frequency bands are fused, respectively.

Step - 4: The resultant fused image is constructed by performing an inverse DWT on the fused coefficient of the above step.

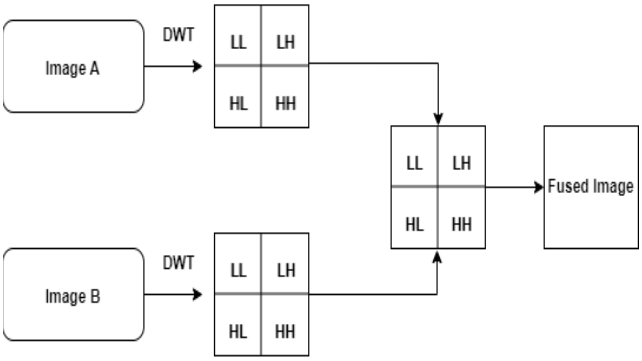

Figure 2. Fusion of various frequency band after frequency decomposition

The schematic flow chart of the implemented DWT based approach is described in given below Figure 03.

Experimental Setup

The details of hardware platform, software platform and dataset used in the work is as under:

Input Image: Registered CT and MRI T1 Images of the lumbar spine having dimensions of 512*512

Dataset Used: Three cases from data set - 1 of "SpineWeb"[46].

Hardware & Software Platform Used: Ryzen 7 3.3GHz, 16GB DDR4 RAM, 6GB NVIDIA Graphics Memory & *MATLAB ver. R2020b* (Image Processing Toolbox & Statistics Toolbox)

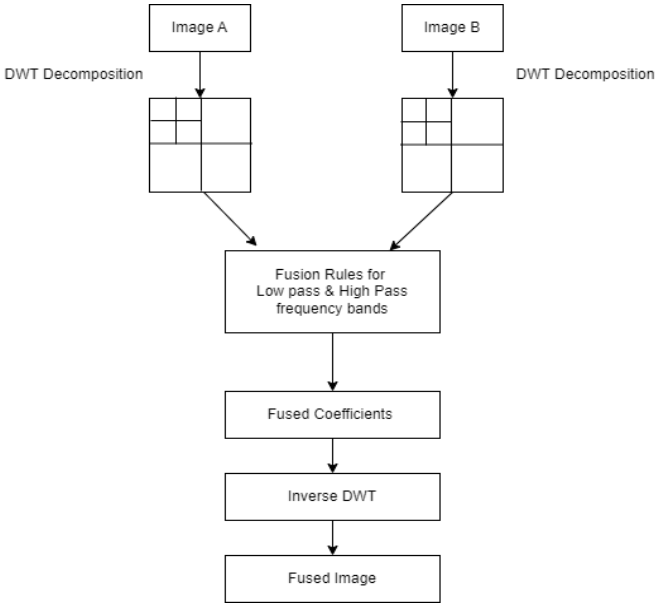

Figure 3. Flow chart of Image Fusion using Discrete Wavelet Transform

Image Registration and Fusion

A CT image is assumed to be a moving image, and MR image is considered a reference image or fixed image for image registration. A landmark control point based image registration technique is implemented to geometrically align CT and MR images with each other. Figure 04 refers to the basic process of image registration performed in this work. Figures 04(a) and (b) are the pre-processed source images from the dataset; Figures 04(c) and (d) represent the marking of landmark points on the source image for registration purposes; and Figure 04(e) represents the registered CT image with respect to the MR image using the landmark point registration process. In the image fusion process, Figures 04 (b) and (e) are considered input images to the algorithm as they are geometrically aligned with each other post registration.

Discrete Wavelet Transform (DWT) has been implemented fusion, and it has been tested for conditions such as (i) different wavelets used for decomposition like 'bior2.2', 'coif', 'db1', 'db2', 'db4'and 'sym4' (ii) levels of decomposition, n = 1, 2, 3 and 4. The image fusion algorithm using DWT is applied to the dataset, but due to space limitations, only three cases are presented in this work.

Image Fusion Rules – Low pass band

The low frequency band is often referred to as the coarser level representation of the original input image, also it is also a smoother and sub sampled version of the input image. Based on the characteristics of CT and MR images, for the fusion of low frequency bands the average rule is used. It takes the average of the absolute wavelet coefficient at each location from the input images as the coefficient at that location in the fused image.

Image Fusion Rules – High pass band

The goal of image fusion is to effectively preserve all necessary information in each input image, such as edges and textures. In an image where the useful features are generally larger than a pixel, pixel-by-pixel fusion may not be appropriate to preserve the necessary information from the input image. For the fusion of high-pass bands, the max select rule with consistency check proposed by Li et.al.[1] is used, which effectively checks that the dominant features are incorporated into the fused image.

Metrics of Quantitative Analysis:

It is a tough task to evaluate the quality of the output fused image when the reference image is not available for comparison. In the past decade, many metrics have been proposed to judge quality, but none of them is universally accepted as a gold standard evaluation metric.[47,48] Hence, it is necessary to evaluate various metrics to summarize any study. The experimental results obtained after the implementation of the image fusion algorithm under different testing conditions are evaluated using widely used quality metrics such as Entropy, Total Mutual Information, $Q^{AB/F}$, and Spatial Frequency. The final output fused image is considered "F" and the input images are considered as "A" and "B" respectively, for all equations mentioned below. The summary of each metric is mentioned below:

(1) Entropy: The entropy of a fused image is defined as

$$\boldsymbol{E = -\sum_{l=0}^{L-1} p_F(l) log_2 p_F(l)} \qquad (1)$$

where L is the number of gray levels for 8-bit images used in this work it is 256 and pF(l) is the normalized histogram of the fused image. Entropy is basically the amount of information in the fused image.

(2) Total Mutual Information:

The total mutual Information is defined as the summation of the mutual information of the fused Image with respect to Image A and the mutual information of the fused image with respect to Image B.

$$\boldsymbol{Total\ Mutual\ Information = MI_{AF} + MI_{BF}} \qquad (2)$$

where MI_{AF} [40] can be calculated as follows

$$\boldsymbol{MI_{AF} = \sum_{af} p_{AF}(a,f) log \frac{p_{AF(a,f)}}{p_A(a) p_F(f)}} \qquad (3)$$

where $p_{AF}$is the joint normalized histogram of A and F, p_A and $p_F$are normalized histograms of image A and F respectively. Similarly the MI_{BF} can also be computed by replacing source image A with image B in the above Equation 3. In the result tables Total Mutual Information is referred as Mutual Information.

(3) $Q^{AB/F}$:

The metric $Q^{AB/F}$[41] is defined as

$$\boldsymbol{Q^{AB/F} = \frac{\sum_{n=1}^{N}\sum_{m=1}^{M}(Q^{AF}(n,m)w^A(n,m) + (Q^{BF}(n,m)w^B(n,m))}{\sum_{n=1}^{N}\sum_{m=1}^{M}(w^A(n,m) + w^B(n,m))}} \qquad \textbf{(4)}$$

Where$Q^{AF}(n,m) = Q_g^{AF}(n,m)Q_\propto^{AF}(n,m)$;

$Q_g^{AF}(n,m)$ *and* $Q_\propto^{AF}(n,m)$are the edge strength and preserve values from orientation respectively. *N* and *M* are the size of images respectively and *n* and *m* represent the image location. $Q^{BF}(n,m)$ is similar to that of $Q^{AF}(n,m)$ by changing the source image as B.

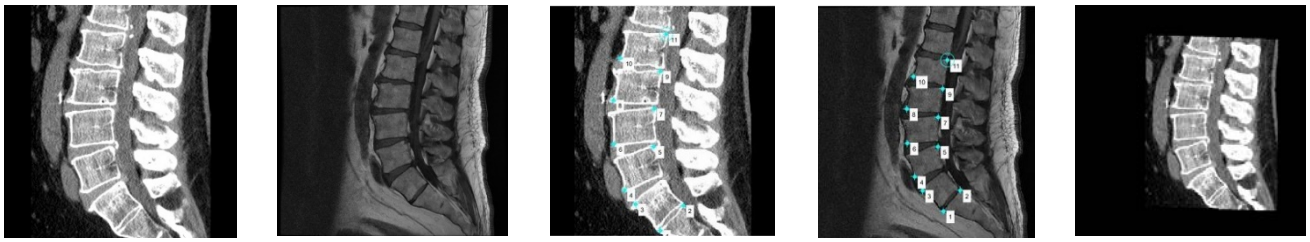

(a) **(b)** **(c)** **(d)** **(e)**

Figure. 04 (a) Source CT Image of Case – 1 (b) Source MR-T1 Image of Case – 1 (c) Landmark points marked on Source CT image for registration with MR – T1 (d) Corresponding landmark points on MR-T1 image (e) Registered CT image with respect to MR-T1 Image

Quality Metrics for Case – 1

Table 01. Entropy & Mutual Information for Case – 1 for different level of decomposition using various wavelets

Wavelet	Entropy – at Decomposition Level				Mutual Information – at Decomposition Level			
	1	2	3	4	1	2	3	4
Bior 2.2	5.4033	5.4312	5.4645	5.4268	***3.4951***	3.1227	2.8558	2.4305
Coif	5.4046	5.4385	5.4708	5.4566	3.4506	3.0842	2.8050	2.3850
Db1	5.4129	5.4354	5.4368	5.3924	3.3910	3.1275	2.9049	2.7047
Db2	5.4051	5.4350	5.4684	5.4480	3.4411	3.0895	2.7690	2.3198
Db4	5.4035	5.4334	5.4596	***5.6115***	3.4670	3.0188	2.6559	2.1417
Sym4	5.4045	5.4329	5.4675	5.4519	3.4697	3.0986	2.8103	2.3123

Table 02. $Q^{AB/F}$& Spatial Frequency for Case – 1 for different level of decomposition using various wavelets

Wavelet	$Q^{AB/F}$ – at Decomposition Level				Spatial Frequency – at Decomposition Level			
	1	2	3	4	1	2	3	4
Bior 2.2	0.5684	0.6275	0.6536	0.6317	7.1734	8.5351	9.1800	9.3794
Coif	0.5655	0.6151	0.6274	0.5925	7.2674	8.6971	9.3453	9.5773
Db1	0.5757	0.6546	0.7018	***0.7066***	7.7713	9.3485	10.1497	***10.4699***
Db2	0.5641	0.6170	0.6264	0.5940	7.3467	8.6317	9.2470	9.4856
Db4	0.5351	0.5790	0.5916	0.5117	7.0054	8.4461	9.1268	9.3706
Sym4	0.5519	0.6089	0.6294	0.5913	7.1873	8.5151	9.1693	9.4094

Quality Metrics for Case – 2

Table 03. Entropy & Mutual Information for Case – 2 for different level of decomposition using various wavelets

Wavelet	Entropy – at Decomposition Level				Mutual Information – at Decomposition Level			
	1	**2**	**3**	**4**	**1**	**2**	**3**	**4**
Bior 2.2	6.8079	6.9208	6.9781	7.0109	***3.4794***	3.1851	2.9991	2.7158
Coif	6.8083	6.9221	6.9850	7.0199	3.4240	3.1618	2.9602	2.6852
Db1	6.8284	6.9303	6.9825	***7.0226***	3.3830	3.2093	3.1178	2.9955
Db2	6.8114	6.9205	6.9746	7.0006	3.4081	3.1490	2.9626	2.6473
Db4	6.7961	6.9180	6.9763	6.9978	3.4643	3.1087	2.8815	2.5055
Sym4	6.8024	6.9179	6.9791	7.0157	3.4561	3.1660	2.9608	2.6561

Table 04. $Q^{AB/F}$& Spatial Frequency for Case – 2 for different level of decomposition using various wavelets

Wavelet	$Q^{AB/F}$– at Decomposition Level				Spatial Frequency – at Decomposition Level			
	1	2	3	4	1	2	3	4
Bior 2.2	0.5001	0.6197	0.6717	0.6714	10.6739	13.0592	13.9311	14.2204
Coif	0.4947	0.6071	0.6398	0.6311	10.8613	13.3399	14.3093	14.6470
Db1	0.5218	0.6465	0.7056	***0.7184***	11.9003	14.4231	15.4124	***15.8332***
Db2	0.4919	0.6087	0.6488	0.6426	10.8894	13.3498	14.2789	14.5993
Db4	0.4460	0.5821	0.6187	0.6176	10.2076	12.9358	13.8443	14.1356
Sym4	0.4744	0.6065	0.6441	0.6414	10.5595	13.0699	13.9865	14.3025

Quality Metrics for Case – 3

Table 05. Entropy & Mutual Information for Case – 3 for different level of decomposition using various wavelets

Wavelet	Entropy – at Decomposition Level				Mutual Information – at Decomposition Level			
	1	**2**	**3**	**4**	**1**	**2**	**3**	**4**
Bior 2.2	5.3978	5.4222	5.4251	5.4299	3.5968	3.1049	2.7739	2.4009
Coif	5.4017	5.4258	5.4315	5.4156	3.5350	3.0592	2.7233	2.3538
Db1	5.4002	5.4006	5.3807	5.3341	3.4420	3.0768	2.8312	2.6139
Db2	5.4010	5.4227	5.4329	5.4139	3.5228	3.0575	2.6948	2.3167
Db4	5.4009	5.4318	5.4574	***5.5292***	***3.6181***	3.0311	2.6330	2.2164
Sym4	5.4004	5.4277	5.4439	5.4408	3.5953	3.0796	2.7339	2.3412

Table 06. $Q^{AB/F}$& Spatial Frequency for Case – 3 for different level of decomposition using various wavelets

Wavelet	$Q^{AB/F}$ – at Decomposition Level				Spatial Frequency – at Decomposition Level			
	1	**2**	**3**	**4**	**1**	**2**	**3**	**4**
Bior 2.2	0.5967	0.6683	0.7002	0.7029	7.4003	8.8305	9.4602	9.6668
Coif	0.5911	0.6555	0.6722	0.6632	7.5129	8.9925	9.6337	9.8398
Db1	0.6051	0.6950	0.7460	***0.7616***	8.0859	9.6971	10.3785	***10.6553***
Db2	0.5901	0.6565	0.6756	0.6676	7.5392	8.9840	9.6344	9.8329
Db4	0.5597	0.6260	0.6457	0.6289	7.1990	8.7671	9.4118	9.5937
Sym4	0.5770	0.6499	0.6774	0.6767	7.3189	8.8105	9.4671	9.6829

Table 07. Quality metrics comparison for all the cases at level of decomposition '4' using various wavelet

	Metrics	Bior2.2	Coif	Db1	Db2	Db4	Sym4
Case - 1	$Q^{AB/F}$	0.6317	0.5925	***0.7066***	0.5940	0.5117	0.5913
	Spatial Frequency	9.3794	9.5773	***10.4699***	9.4856	9.3706	9.4094
	Entropy	5.4268	5.4566	5.3924	5.4480	***5.6115***	5.4519
	Mutual Information	2.4305	2.3850	***2.7047***	2.3198	2.1417	2.3123
Case -2	$Q^{AB/F}$	0.6714	0.6311	***0.7184***	0.6426	0.6176	0.6414
	Spatial Frequency	14.2204	14.6470	***15.8332***	14.5993	14.1356	14.3025
	Entropy	7.0109	7.0199	***7.0226***	7.0006	6.9978	7.0157
	Mutual Information	2.7158	2.6852	***2.9955***	2.6473	2.5055	2.6561
Case - 3	$Q^{AB/F}$	0.7029	0.6632	***0.7616***	0.6676	0.6289	0.6767
	Spatial Frequency	9.6668	9.8398	***10.6553***	9.8329	9.5937	9.6829
	Entropy	5.4299	5.4156	5.3341	5.4139	***5.5292***	5.4408
	Mutual Information	2.4009	2.3538	***2.6139***	2.3167	2.2164	2.3412

$w^A(n,m)$ & $w^B(n,m)$ represent the importance of $Q^{AF}(n,m)$ & $Q^{BF}(n,m)$ respectively.

(4) Spatial Frequency: The spatial frequency is defined as the amount of frequency content present in the image. Also, it indicates the sharpness or clarity of the image.

RESULT ANALYSIS

For experimental analysis, various wavelets with different values of decomposition, i.e., 1, 2, 3, and 4, were implemented for image fusion of CT and MR images. Due to space constraints, the results of 3 cases are presented in the form of a table, out of which 1 case is presented with fused output images. The outcome of all wavelet-based image fusion algorithms for different decomposition values was evaluated by the quality metrics described in the previous section

Tables 01 to 06 below describe the quality metrics of three different cases taken from the Spine web dataset and evaluated in this study; table 07 represents the comparison of metrics for all the implemented wavelets at level '4' of decomposition; and Figure 05 refers to the output fused image by applying different wavelets and selecting the different levels of decomposition. The numbers, which are bold and in italics, represent the best performance of particular quality metrics.

The given figure 05 represents the output fused image of one case using discrete wavelet transform for all wavelet families and decomposition level. Upon analysis of quality metrics of three cases taken from the 'Spine Web' dataset in this study, the following things can be summarized:

Overall it was observed that metrics such as Entropy, $Q^{AB}/_F$, and Spatial frequency of output fused images are directly proportional to the level of decomposition which means the higher the level of decomposition higher the value metric for the respective wavelet type.

In the case of mutual information, it followed the reverse trend compared to other metrics, i.e., as the level of decomposition increases, the metric value decreases, which implies an inverse proportional behavior of the metric with the decomposition value for the respective wavelet type.

For Case 1 – among all the implemented wavelets, it was observed that the best performance in regards to (i) Entropy was observed in db4 type wavelet for level 4 (ii) Mutual Information in bior2.2 type for level 1 (iii) $Q^{AB}/_F$ in db1 type for level 4 and (iv) Spatial frequency in db1 type for level 4.

For Case 2 – among all the implemented wavelets, it was observed that the best performance in regards to: (i) Entropy was observed in the db1 type wavelet for level 4 (ii) Mutual Information in bior2.2 type for level 1 (iii) $Q^{AB}/_F$ in db1 type for level 4 and (iv) Spatial Frequency in db1 type for level 4.

For Case 3 – among all the implemented wavelets, it was observed that the best performance in regards to: (i) Entropy was observed in the db4 type wavelet for level 4 (ii) Mutual Information in db4 type for level 1 (iii) $Q^{AB}/_F$in db1 type for level 4 and (iv) Spatial Frequency in db1 type for level 4. It is very clear that for a lower value of decomposition level, it implies less presence of spatial details, and if the level of decomposition is set too high, then there are always chances of fusion error as the output of the high pass band is highly dependent on noise sensitivity and misregistration error. Hence, a trade-off needs to be made to select the decomposition level where the output fused image covers necessary spatial details and is also not sensitive to mis-registration.

Entropy (E) indicated the overall information present in any image, it was observed that the highest value was obtained for the 4th level of decomposition, and in cases 1 and 3, it was recorded for the "db4" wavelet, and in case 2, it was for the "db2" wavelet.

Mutal information(MI) as described in the previous section, indicates the amount of information from the source image that is retained in the fused image. It was also observed in the case of mutual information, having inverse behavior in performance in regards to level of decomposition, and the best metric was obtained in 'bior2.2' for the first two cases and 'db4' in the third case as decomposition level 1. But considering the decomposition level as '4, it was noted that in the case of mutual information, 'db1' has performed best in all the cases.

The higher the value of Spatial freqeuncy (SF) it indicates the overall quality of fused image is more and in the case of $Q^{AB}/_F$, the higher value indicates it is able to preserve more edge level information. It was observed that for both the metrics the highest value was observed for "4" level of decomposition in "db1" wavelet which indicates the good quality of fused image with edge presevation from source images.

Considering the level of decomposition as '4, it was observed that in all three presented cases, the db1' wavelet type outperformed in the majority of metrics except for a few instances where Entropy was found to be best in 'db4' in two cases.

SUMMARY

The main goal of image fusion is to combine complementary information from different input images and produce a single output image with more information. This study implemented various types of wavelets and tested for different values of decomposition. The performance of the implemented algorithm was analyzed using various quality metrics for each wavelet and decomposition level.

Overall, it can be summarized that level "4" of decomposition was found to be appropriate for image fusion considering the various factors mentioned and results summarized; the same has also been summarized in the litreature.[49,50]

Also, the "db1" wavelet achieved comparable performance in terms of quality metrics compared to its counterpart wavelets. The main goal of image fusion is to increase the accuracy of diagnosis and assist clinicians in decision-making.

In the future, this work can be expanded by focusing on the implementation of different wavelet families for level 4 composition on a larger dataset, with the end goal of using fused images towards the development of a decision support system for the analysis of spine-related disorders.

CONFLICTS OF INTEREST

The author(s) declare(s) that there is no conflict of interest regarding the publication of this paper.

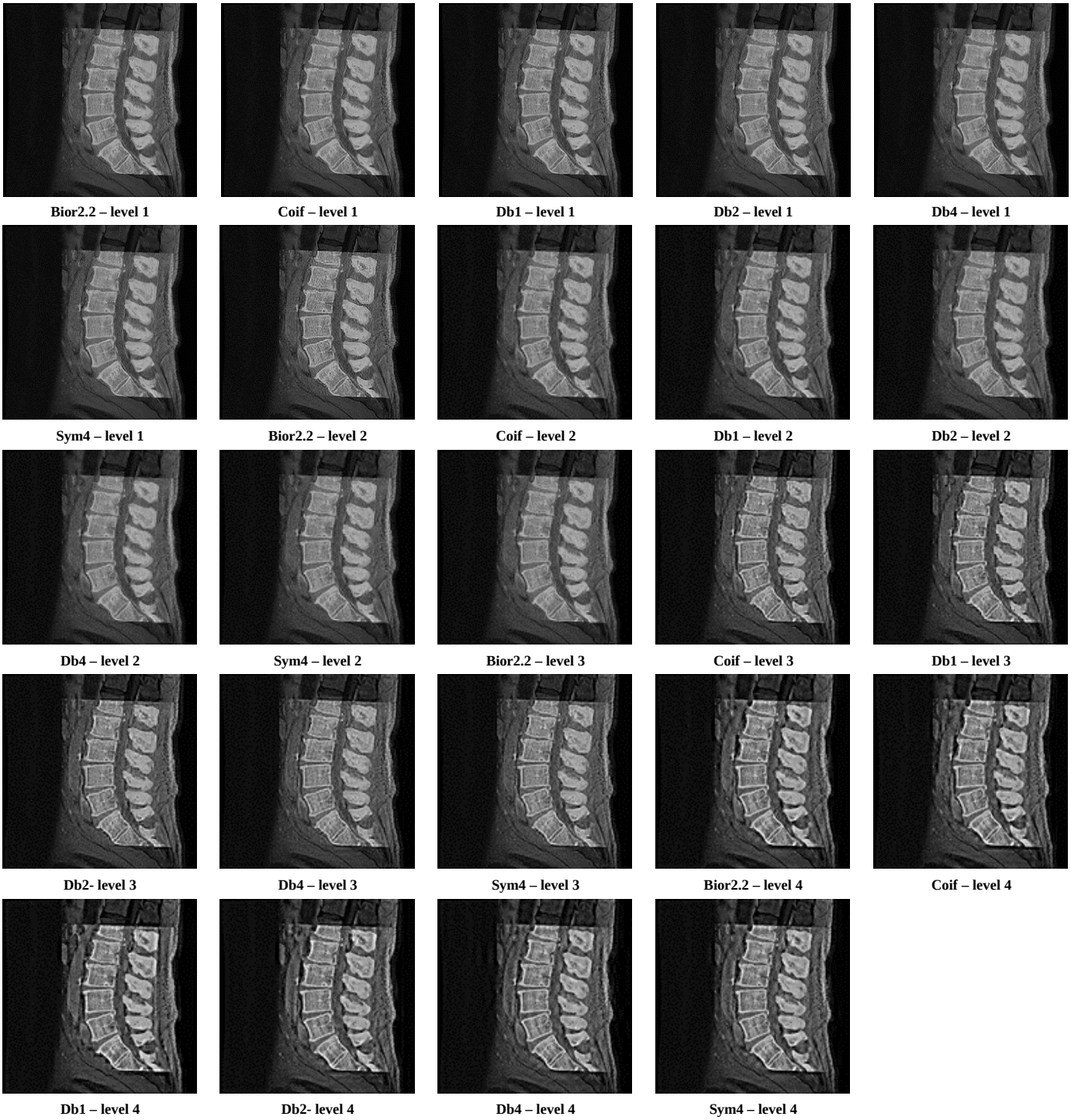

Figure. 05 Output Fused image for different wavelets and different values of decomposition (Label Prefix is "Name of Wavelet" followed by level of decomposition

REFERENCES

1. H. Li, B.S. Manjunath, S.K. Mitra. Multisensor image fusion using the wavelet transform. *Graphical models and image processing* **1995**, 57 (3), 235–245.
2. M. El-Bassiouni, I.F. Ciernik, J.B. Davis, et al. [18FDG] PET-CT-based intensity-modulated radiotherapy treatment planning of head and neck cancer. *International Journal of Radiation Oncology* Biology* Physics* **2007**, 69 (1), 286–293.
3. A. Wong, W. Bishop. Efficient least squares fusion of MRI and CT images using a phase congruency model. *Pattern Recognition Letters* **2008**, 29 (3), 173–180.
4. Liu, Q. Wang, Y. Shen. Comparisons of several pixel-level image fusion schemes for infrared and visible light images. In *2005 IEEE*

Instrumentationand Measurement Technology Conference Proceedings; IEEE, **2005**; Vol. 3, pp 2024–2027.
5. R. Wang, F. Bu, H. Jin, L. Li. A feature-level image fusion algorithm based on neural networks. In *2007 1st international conference on bioinformatics and biomedical engineering*; IEEE, **2007**; pp 821–824.
6. S. Prabhakar, A.K. Jain. Decision-level fusion in fingerprint verification. *Pattern Recognition* **2002**, 35 (4), 861–874.
7. L. Song, Y. Lin, W. Feng, M. Zhao. A novel automatic weighted image fusion algorithm. In *2009 International Workshop on Intelligent Systems and Applications*; IEEE, **2009**; pp 1–4.
8. J.R. Harris, R. Murray, T. Hirose. IHS transform for the integration of radar imagery with other remotely sensed data. *Photogrammetric Engineering and Remote Sensing* **1990**, 56 (12), 1631–1641.
9. V.P.S. Naidu, J.R. Raol. Pixel-level image fusion using wavelets and principal component analysis. *Defence Science Journal* **2008**, 58 (3), 338.
10. A.R. Gillespie, A.B. Kahle, R.E. Walker. Color enhancement of highly correlated images. II. Channel ratio and "chromaticity" transformation techniques. *Remote Sensing of Environment* **1987**, 22 (3), 343–365.
11. S. Kumari, M. Malviya, S. Lade. Image fusion techniques based on pyramid decomposition. *International Journal of Artificial Intelligence and Mechatronics* **2014**, 2 (4), 127–130.
12. S. Singh, N.S. Grewal, H. Singh. Multi-resolution representation of multifocus image fusion using Gaussian and Laplacian pyramids. *Int J Adv Res Comput Sci Softw Eng* **2013**, 3 (11), 1639–1642.
13. P.J. Burt, E.H. Adelson. The Laplacian pyramid as a compact image code. In *Readings in computer vision*; Elsevier, **1987**; pp 671–679.
14. H. Olkkonen, P. Pesola. Gaussian pyramid wavelet transform for multiresolution analysis of images. *Graphical Models and Image Processing* **1996**, 58 (4), 394–398.
15. P.J. Burt. A gradient pyramid basis for pattern-selective image fusion. *Proc. SID 1992* **1992**, 467–470.
16. A. Toet. Image fusion by a ratio of low-pass pyramid. *Pattern Recognition Letters* **1989**, 9 (4), 245–253.
17. R. Singh, A. Khare. Multiscale medical image fusion in wavelet domain. *The Scientific World Journal* **2013**, 2013.
18. G. Pajares, J.M. De La Cruz. A wavelet-based image fusion tutorial. *Pattern recognition* **2004**, 37 (9), 1855–1872.
19. C. Burrus, R. Gopinath, H. Guo. Introduction to Wavelets and Wavelet Transform—A Primer. *Recherche* **1998**, 67.
20. M. Unser, T. Blu. Wavelet theory demystified. *IEEE Transactions on Signal Processing* **2003**, 51 (2), 470–483.
21. V.P.S. Naidu. Discrete cosine transform based image fusion techniques. *Journal of Communication, Navigation and Signal Processing* **2012**, 1 (1), 35–45.
22. S. Krishnamoorthy, K.P. Soman. Implementation and comparative study of image fusion algorithms. *International Journal of Computer Applications* **2010**, 9 (2), 25–35.
23. S. Udomhunsakul, P. Yamsang, S. Tumthong, P. Borwonwatanadelok. Multiresolution edge fusion using SWT and SFM. In *Proceedings of the World Congress on Engineering*; **2011**; Vol. 2, pp 6–8.
24. P. Borwonwatanadelok, W. Rattanapitak, S. Udomhunsakul. Multi-focus image fusion based on stationary wavelet transform and extended spatial frequency measurement. In *2009 international conference on electronic computer technology*; IEEE, **2009**; pp 77–81.
25. H. Zhou. An stationary wavelet transform and curvelet transform based infrared and visible images fusion algorithm. *International Journal of Digital Content Technology and its Applications* **2012**, 6 (1).
26. S. Li, X. Kang, L. Fang, J. Hu, H. Yin. Pixel-level image fusion: A survey of the state of the art. *Information Fusion* **2017**, 33, 100–112.
27. F.E.-Z.A. El-Gamal, M. Elmogy, A. Atwan. Current trends in medical image registration and fusion. *Egyptian Informatics Journal* **2016**, 17 (1), 99–124
28. A.P. James, B.V. Dasarathy. Medical image fusion: A survey of the state of the art. *Information Fusion* **2014**, 19, 4–19.
29. S. Bhat, D. Koundal. Multi-focus image fusion techniques: a survey. *Artificial Intelligence Review* **2021**, 54, 5735–5787.
30. S. Cheng, J. He, Z. Lv. Medical Image of PET/CT Weighted Fusion Based on Wavelet Transform. In *2008 2nd International Conference on Bioinformatics and Biomedical Engineering*; **2008**; pp 2523–2525.
31. Q. Nawaz, B. Xiao, I. Hamid, D. Jiao. Multi-modal Color Medical Image Fusion Using Quaternion Discrete Fourier Transform. *Sensing and Imaging* **2016**, 17 (1), 7.
32. C.T. Kavitha, C. Chellamuthu, R. Rajesh. Medical Image Fusion using Combined Discrete Wavelet and Ripplet Transforms. *Procedia Engineering* **2012**, 38, 813–820.
33. A.R. Doke, T. Singh, K. Shantanu, R. Nayar. Comparative analysis of wavelet transform methods for fusion of CT and PET images. In *2017 IEEE International Conference on Power, Control, Signals and Instrumentation Engineering (ICPCSI)*; **2017**; pp 2152–2156.
34. B. Zitová, J. Flusser. Image registration methods: a survey. *Image and Vision Computing* **2003**, 21 (11), 977–1000.
35. M. Balci. Sub-pixel registration in computational imaging and applications to enhancement of maxillofacial CT data. **2006.**
36. T.M. Lehmann, H.-G. Gröndahl, D.K. Benn. Computer-based registration for digital subtraction in dental radiology. *Dentomaxillofacial Radiology* **2014.**
37. F. Alam, S.U. Rahman. INTRINSIC REGISTRATION TECHNIQUES FOR MEDICAL IMAGES: A STATE-OF-THE-ART REVIEW. *JPMI: Journal of Postgraduate Medical Institute* **2016**, 30 (2).
38. H. Irshad, M. Kamran, A.B. Siddiqui, A. Hussain. Image fusion using computational intelligence: A survey. In *2009 Second International Conference on Environmental and Computer Science*; IEEE, **2009**; pp 128–132.
39. R. Maruthi, I. Lakshmi. Multi-focus image fusion methods–a survey. *Comput Eng* **2017**, 19 (4), 9–25.
40. B. Meher, S. Agrawal, R. Panda, A. Abraham. A survey on region based image fusion methods. *Information Fusion* **2019**, 48, 119–132
41. K. Rani, R. Sharma. Study of different image fusion algorithm. *International journal of Emerging Technology and advanced Engineering* **2013**, 3 (5), 288–291.
42. Q. Guo, F. Dong, S. Sun, B. Lei, B.Z. Gao. Image denoising algorithm based on contourlet transform for optical coherence tomography heart tube image. *IET image processing* **2013**, 7 (5), 442–450.
43. C.K. Solanki, N.M. Patel. Pixel based and Wavelet based Image fusion Methods with their Comparative Study. In *National conference on recent trends in engineering & technology*; **2011**; Vol. 13, pp 13–14.
44. H. Wang, H. Xing. Multi-mode medical image fusion algorithm based on principal component analysis. In *2009 International Symposium on Computer Network and Multimedia Technology*; IEEE, **2009**; pp 1–4.
45. N. Al-Azzawi, W. Abdullah. Medical image fusion schemes using Contourlet transform and pca bases. *Image fusion and its applications* **2011**, 93–110
46. 'Spineweb online database'. Available at http://spineweb.digitalimaginggroup.ca
47. P. Yan. Information measure for performance of image fusion. *Electronics Letters* **2002**, 38 (7), 313-315(2).
48. C.S. Xydeas, V.S. Petrovic. Objective image fusion performance measure. *Electronics Letters* **2000**, 36, 308–309.
49. S. Li, B. Yang, J. Hu. Performance comparison of different multi-resolution transforms for image fusion. *Information Fusion* **2011**, 12 (2), 74–84.
50. Y. Parikh, H. Koringa. Left Ventricle Segmentation using Bidirectional Convolution Dense Unet. *J. Integr. Sci. Technol.* **2023**, 11 (1), 417.